



Research Article

Development of the Low-Economic-Risk Microgrids to Establish Environmental-Friendly Industries

Mohammad Hossein Jahangir*, Arash Kargarzadeh, Mohammad Montazeri

Department of Renewable Energies and Environment, Faculty of New Science and Technologies, University of Tehran, P. O. Box: 1439957131, Tehran, Tehran, Iran.

PAPER INFO

Paper History:

Received: 26 February 2022

Revised: 18 June 2022

Accepted: 29 June 2022

Keywords:

Micro Grid,
Green Factory,
Carbon Emission,
Deferrable Load,
Economic Analysis

ABSTRACT

As one of the main consumers of electricity, industries account for in releasing a large amount of emission. Using renewable energies to feed factories is not an easy task and they should be economically viable to compete with fossil fuels. The goal of this study is to analyze the possibilities of using energy local area networks in off-grid and on-grid modes in an industrial project by considering and calculating all primary and deferrable loads in detail for the first time. The industrial project is sensitive and all possibilities should be considered closely to avoid economic losses. In this case, changes in electrical loads during the project, degradation of components, environmental risks, and economic risks of the investment (for each scenario) are considered and determined too. The results indicate that component degradation can cause 24,000 kWh drop in total electricity production at the end of the project and the total biogas consumption increases from 742 kg/yr to 9330 kg/yr. The results also show that the on-grid scenario (solar/battery) with the Net Present Cost of 200,000\$ will be an easy and low-risk choice for investment, but has high environmental risks. On the other hand, the stand-alone scenario (solar/wind/bio/battery) with Net Present Cost of 598,000\$ minimizes the environmental risks at the expense of high investment risk. A proper comparison between the multi-year and single-year modes at the end of the project ensures the high accuracy of techno-economic analysis in terms of optimum system types, emissions, and economics.

<https://doi.org/10.30501/jree.2022.330754.1338>

1. INTRODUCTION

Renewable energies and hybrid systems have been developing in recent years and research on their possibilities is growing in scope. Most studies addressing these systems are validated by HOMER (Hybrid Optimization of Model with Multiple Energy Resources) pro software enjoying the ability to simulate multiple systems together and to optimize them [1]. Microgrids are more reliable and cheaper than single energy systems and can be installed in regions without access to grid power like rural regions [2]. Table 1 shows detailed information and results of recent techno-economic studies over hybrid renewable energy systems.

The use of hybrid energy systems for factories and industrial projects is on the rise recently as industries are one the largest producers of emissions [10]. Table 2 shows economic, technical, and environmental information of recent researches over establishing green factories.

However, failing to consider the effects of inflation rate and discount rate fluctuations, almost all studies on establishing green factories did not predict the effects of development of

the factory that may change the electrical load and none of them considered the degradation of installed components during the project lifetime. The goal of this paper is to introduce an accurate plan for establishing green industries. This study attempts to consider and determine the effects of fluctuations in inflation and discount rates on the most important economic and environmental parameters of an industrial project using sensitivity analysis of HOMER pro software. This will show the amount of both economic and environmental risks of establishing green factories for different scenarios. Moreover, for the first time, the deferrable load of an industrial factory will be considered and determined in detail along with the effects of photovoltaic panel degradation and changes in electrical loads during the project using multi-year module of HOMER pro software. This will encourage factory managers around the world to use hybrid renewable energy systems and save the environment while investing their money in a safe project.

2. CASE STUDY

2.1. Factory information

The adopted case study is a factory that manufactures the needed machinery for petrochemical industries. The factory is

*Corresponding Author's Email: mh.jahangir@ut.ac.ir (M.H. Jahangir)
URL: https://www.jree.ir/article_155103.html



located in Shamsabad Industrial town in Tehran, Iran. The area where factory is located is 2450 m² and its main structure is 1000 m². There is also a technical department featuring the area of 120 m² and a parking area with 45m². Figure 1 shows details of the factory area in a map.

2.2. Electrical load

The factory has a primary electrical load mainly derived from industrial machines. There is also a deferrable load which is available due to use of water pumps and air compressors.

2.2.1. Primary load

Table 3 shows the consumption values for the past three years and explains how much they increase after each year. The primary electrical load profile is also shown in Figure 2 in detail.

According to Figure 2, the maximum monthly peak load is 165 kW and the daily peak load is 90 kW.

Table 1. Detailed information and results of recent findings over hybrid renewable energy systems

Location	Load type	Year	Grid	System	Results	Ref.
Tripoli	Electrical	2020	Off	PV ² /FC ³ /Bat ⁴	It was found that hybridizing photovoltaic panels with fuel cells ensured a better minimum threshold power of 5 kW than solar thermal energy and fuel cells.	[3]
China	Electrical	2020	Off	PV/WT ⁵ //HSPSI ⁶	A real hybrid renewable energy system that is using pumped-storage system instead of batteries was studied, which indicated that such systems could considerably reduce the capital cost and PV/WT/HSPSI was the most cost-effective combination.	[4]
Honduras	Electrical	2021	On	PV/bio/Bat	A Gasifier was designed and coupled with PV panels. For the first time, a gasifier was used in HOMER software to simulate a microgrid for rural areas.	[5]
Turkey	Electrical	2021	Both	PV/WT/FC/HE ⁷	HOMER Software was utilized to analyze the penetration levels of resources in both on-grid and off-grid systems in rural regions.	[6]
Mexico	Electrical	2022	Both	PV/WT/FC/Bat	A techno-economic study was done to implement a Hydrogen based Power to Gas to Power (P2G2P) in a microgrid, located in Mexico. This study explains that by using hydrogen and fuel cells to substitute diesel generators, it is possible to reduce CO ₂ emission by 27 %.	[7]
Iran	Electrical	2022	Both	PV/WT/bio/Bat	The paper goal is to reduce the emissions of industrial livestock farms using several microgrids. This study also created a scenario that could help all livestock farms of a country to use their biomass to produce green energy.	[8]
Nepal	Electrical	2022	Off	PV/Diesel	An off-grid microgrid for both Diesel Generators (DG) and solar PV based systems was designed using HOMER. The final DG-based microgrid system reduced fuel consumption by 19 % and costs of the system by 5 %.	[9]

Table 2. Detailed techno-economic-environmental results of recent studies on environmental-friendly industries

Industry	System	NPC (\$)	COE (\$/kWh)	CO ₂ (kg/yr)	Emission desc.	Ref.
Telecom	PV/DG/Bat	401,000	1.28	-60,595	-	[11]
Generic	PV/WT/DG/Bat	1,684,118	0.19	-278,191	Compared with diesel only	[12]
Cement	PV/WT/Bat/Grid	-	0.20	-71,373 Tons	In total	[13]
Cement	PV/BG/Bat	~22 M	0.14	35,731	-	[14]
Dairy	PV/WT/DG/Grid	~14.3 M	0.02	-205,334	Compared with grid only	[15]

² Photovoltaic

³ Fuel Cell

⁴ Battery

⁵ Wind Turbine

⁶ Pumped Storage

⁷ Hydro Electric



Figure 1. Area details of the case study (KSJ factory)

Table 3. Average power consumption of the factory

Year	Ave. monthly consumption (kWh/month)	Ave. daily consumption (kWh/day)	Increase (%)
2019	5201.5	173.4	9 %
2018	4771.5	159.1	14 %
2017	4170	139.0	-

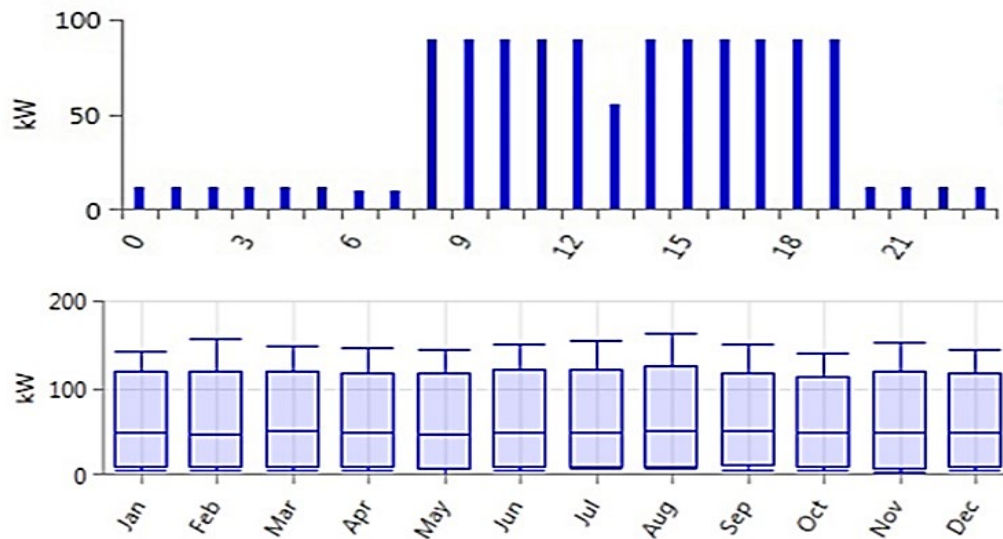


Figure 2. Primary electrical load of the selected factory. (Up: daily load profile, down: seasonal load profile)

2.2.2. Deferrable load

The deferrable load consists of two water pumps and two air compressors. Calculating the deferrable load and its parameters is the next step of the work. The peak load of the deferrable load is equal to load of pumps and compressors and can be easily determined using Eq. 1 in Table 4 [16].

Scaled annual average (kWh/day) is the next needed parameter in this part. HOMER Pro software can automatically determine this number if the user adds the average load of each month [16]. The average time that each of these devices remained operational during all months of one year is measured. Table 5 is available and the scaled

annual average value will therefore be determined automatically.

By setting up the deferrable load chart in HOMER pro software using data available in Table 5, the scaled annual average is determined and reported as 4.34 kWh/day.

Storage capacity calculation represents the last step in completing the data of deferrable load. Storage capacity is

equal to the time when pumps or air compressors need to fill their tanks and it should be reported in kWh [16]. The storage capacity of water pumps is equal to 2.22 kWh. The storage capacity of each compressor is also 0.37 kWh. In this case, the total storage capacity for the deferrable load is equal to 2.96 kWh. Table 6 shows a summary of assumptions and results of storage capacity calculations.

Table 4. Deferrable load equation

Equation	Eq. No.	Ref.
$\Sigma P_{\text{Components}} = \text{Peak Load}$ $P_{\text{pump no.1}} + P_{\text{pump no.2}} + P_{\text{comp. no.1}} + P_{\text{comp. no.2}} = \text{Peak Load}$	1	[16]

Table 5. Information of each available deferrable load in the factory during one year

Month	Ave. operation time (hour)		Ave. consumption (kWh/d)		Total consumption (kWh/d)
	Pumps	Compressors	Pumps	Compressors	
January	2	1.34	0.74	2.95	3.7
February	2	1.34	0.74	2.95	3.7
March	2	1.34	0.74	2.95	3.7
April	1	1	0.37	2.2	2.57
May	2	1.34	0.74	2.95	3.7
June	4	1.67	1.5	3.67	5.17
July	6	1.34	2.2	2.95	5.15
August	7	1.67	2.6	3.67	6.27
September	4	2.5	1.5	5.5	7
October	2	1.34	0.74	2.95	3.7
November	2	1.34	0.74	2.95	3.7
December	2	1.34	0.74	2.95	3.7

Table 6. Assumptions and results of storage capacity calculations

Device	Power (kW)	Quantity	Storage capacity (m ³)	Filling time (hour)	Total storage capacity (kWh)
Water pump	0.37	2	10	3	2.22
Air compressor	2.2	2	0.3	0.17	0.74

3. ENERGY RESOURCES

3.1. Solar energy

Photovoltaic panels can be installed at the roof top of the main structure, technical department, and parking (Figure 1). By considering half of the rooftop of the main structure that faces the sun, the roof of technical department, and parking, 665 m² available space for installing panels is available.

Figure 3 shows the solar GHI and clearness index information of the area where the case study is located. This information is available from NASA website [17].

HOMER software uses Eq. 2 to calculate the output power of photovoltaic panels (Table 7) [18]. where Y_{PV} is the rated capacity of photovoltaic panels, f_{PV} the derating factor, G_T the solar radiation incident, $G_{T,STC}$ solar radiation incident under Standard Test Condition (STC) of photovoltaic panels, α_P the temperature coefficient of PVs available in the data sheet of solar panels, T_C the temperature at which PVs are working, and $T_{C,STC}$ equal to the temperature of the standard test condition of the photovoltaic panels.

Table 7. Out power of PVs equation

Equation	Eq. No.	Ref.
$P_{PV} = Y_{PV} f_{PV} \left(\frac{G_T}{G_{T,STC}} \right) \left(1 + \alpha_P (T_C - T_{C,STC}) \right)$	2	[18]

As shown in Eq. 2, the temperature also affects the efficiency of solar panels and the average daily temperature of the selected environment where the factory is established is gathered using the same method that solar GHI and clearness index were achieved, as shown in Figure 4.

The data of ambient temperature in Figure 4 is employed to calculate the temperature of PVs using Eq. 3 (Table 8) [19].

Table 8. Impact of temperature on PVs equation

Equation	Eq. No.	Ref.
$\alpha_T G_T = U_L (T_C - T_a) + \eta_C G_T$	3	[19]

where α is equal to the solar absorption of the photovoltaic panels, τ is related to the solar transmittance of PVs that belong to the cover that is over them, U_L the coefficient of

heat transfer, T_a the ambient temperature which is available from the data in Figure 4, and η_c belongs to the electrical efficiency of the solar panels.

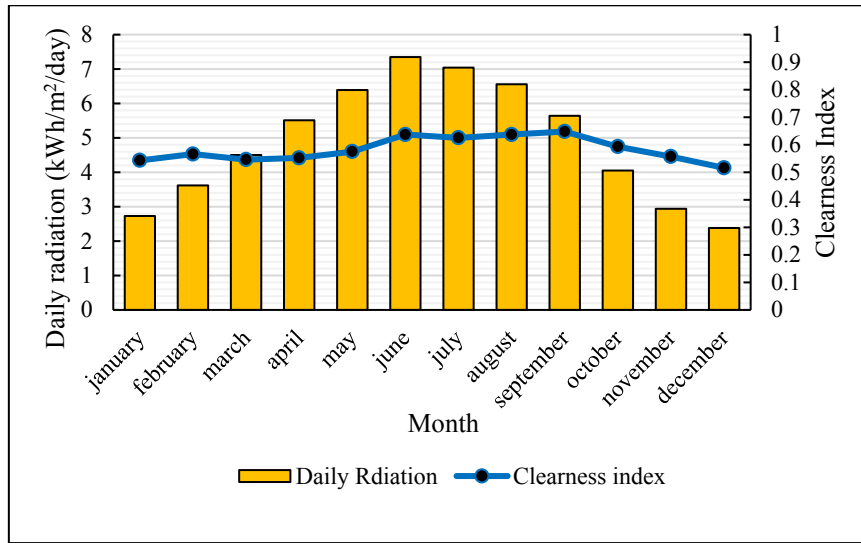


Figure 3. Solar GHI and clearness index of the selected factory’s environment [17]

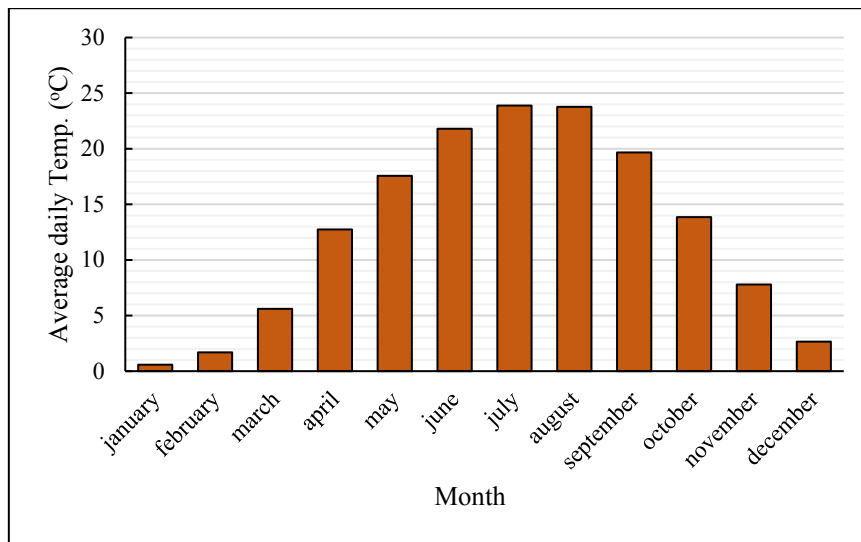


Figure 4. Average daily temperature of the selected factory’s environment

3.2. Wind energy

Given that wind turbines can be operational for 24 hour of the day and produce power, they are necessary components for stand-alone energy hub systems [20]. HOMER pro software uses the power curve of wind turbines to calculate their output power in every time step using the ambient wind data in Figure 5 [21].

In order to determine and achieve the power curve of the wind turbine, Eq. 4 in Table 9 is used for calculating output power of the wind turbine [22].

Table 9. Wind turbine output power equation

Equation	Eq. No.	Ref.
$P_{WT}(t) = \begin{cases} \alpha V^3(t) - \beta P_R & V_{Ci} < V < V_r \\ P_R & V_r < V < V_{Co} \\ 0 & \text{else} \end{cases}$	4	[22]

where V_r belongs to the rated speed, V_{Ci} is equal to the cut-in speed, V_{Co} is related to the cut-off speed, P_R is the rated power of the wind turbine, $\alpha = \frac{P_R}{V_r^3 - V_{Ci}^3}$, and $\beta = \frac{V_{Ci}^3}{V_r^3 - V_{Ci}^3}$.

The wind speed data shown in Figure 5 belong to the 50 m above the surface of the earth. In order to determine the speed of the wind that reaches the blades of wind turbines and calculate the power of the wind turbine (Eq. 4), Eq. 5 is employed (Table 10) [22].

Table 10. Equation of the wind speed which reaches the blades

Equation	Eq. No.	Ref.
$v = v_h \left(\frac{h}{h_r} \right)^Y$	5	[22]

where V is equal to the wind speed at the height of the hub, V_h is the wind speed that is available in Figure 5, h_r is equal to 50 m, h is the hub height, and Y ranges between 0.14 and 0.25.

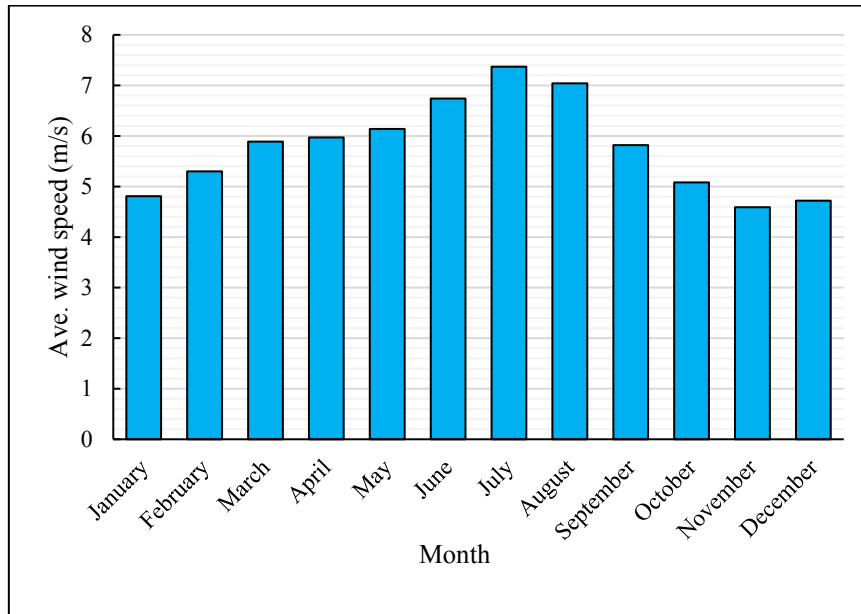


Figure 5. Average wind speed of the selected factory’s environment

3.3. Grid network

Being connected to the grid network gives the system a chance to sell the surplus green energy and provides both economic and environmental profits. There are some hours during the working hours of factory when renewable energies may not be available. In this case, the factory can use grid power to avoid the capacity shortages in grid-connected scenarios. The system will do so at the cost of producing emissions and paying carbon taxes. Emission content values of grid network and carbon taxes are shown in Table 11.

Table 11. Emission penalties and emission contents [23, 24]

Emission	Emission penalties (\$/t)	Emission contents (gr/kWh)
CO ₂	2.86	660.65
CO	54	0.62
SO ₂	521.5	1.66
NO _x	171.5	2.38
Unburnt hydrocarbons	60	180.18
Particulate matter	1228.6	0.12

There is an average of 30 times grid power outage in this industrial town over the course of a year with the average of 2-hour shortage for each one that considerably affects the operations of the factory. Figure 6 shows the grid power outage times in a year.

Grid prices in Iran and the corresponding schedule in different months and hours are also shown in Figure 7 and explained further in Table 12 [24]. Note that charging battery from grid power and also grid sales from battery are not allowed at all.

3.4. Fuel resources

Using generators that consume fuels to produce power is common among factories and they act as backup systems [25]. Fuel resources are always available and can provide enough electricity for energy-local area networks when the renewable energies are not available, but they mostly do so at the expense of producing emissions. The case study of the paper uses a diesel generator to provide electricity during grid outages. Although it is possible to hybrid the diesel power with wind energy, solar energy, and grid power, it should be considered that diesel fuel causes emission and the goal of the paper is to minimize the use of fossil fuels and establish a green factory. In this case, using biofuels instead of diesel is recommended and Biogas (bio-methane) is going to be used instead of diesel fuel in the simulations at a price of 1.1 \$/kg [26]. Biogas produces 60-80 % less greenhouse gas and can provide power for the hybrid energy systems while reducing the emissions [27]. Buying biogas instead of diesel and using it as a backup energy source can also encourage industrial livestock farms to produce green fuels from their produced biomass and help the environment while investing in green energies.

4. COMPONENTS AND SCENARIO

In this part, all technical and economic information of used components is gathered and discussed over. The hybrid renewable energy system that is going to supply the energy demands of this factory was also studied in both off-grid and on-grid modes. Figure 8 shows the schematic of the system and all the components used.

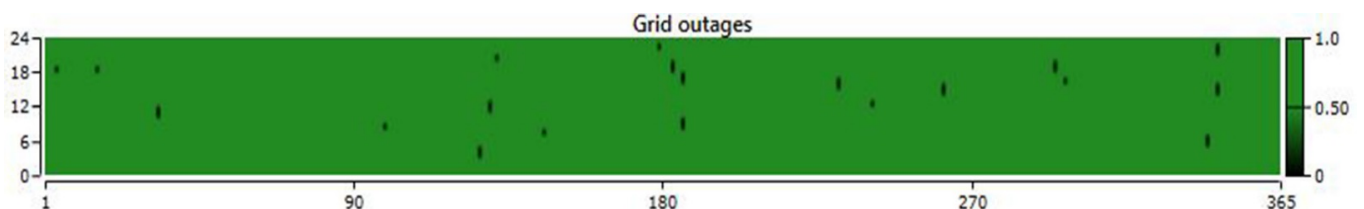


Figure 6. Grid outage times of the industrial town during one year

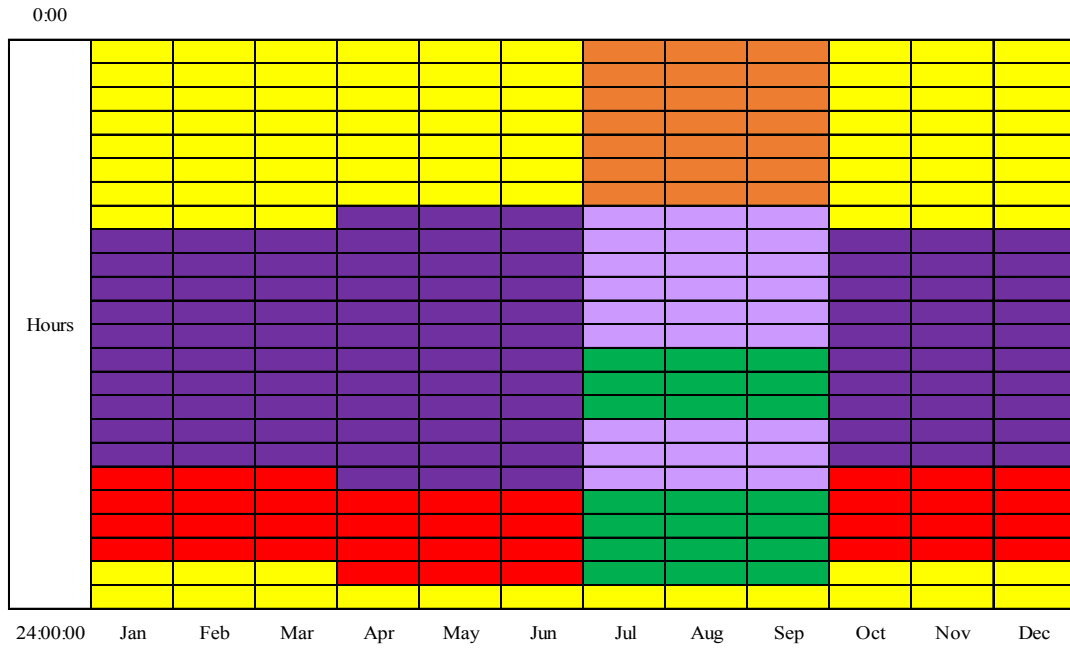


Figure 7. Grid rate schedule of Iran during different hours and months [24]

Table 12. Grid rates and electricity prices of Iran [24]

Rate	Price (\$/kWh)	Color
Low-power-consumption hours in non-summer season	0.05	Yellow
Medium-power-consumption hours in non-summer season	0.07	Purple
High-power-consumption hours in non-summer season	0.10	Red
Low-power-consumption hours in summer season	0.06	Orange
Medium-power-consumption hours in summer season	0.08	Light Purple
High-power-consumption hours in summer season	0.12	Green

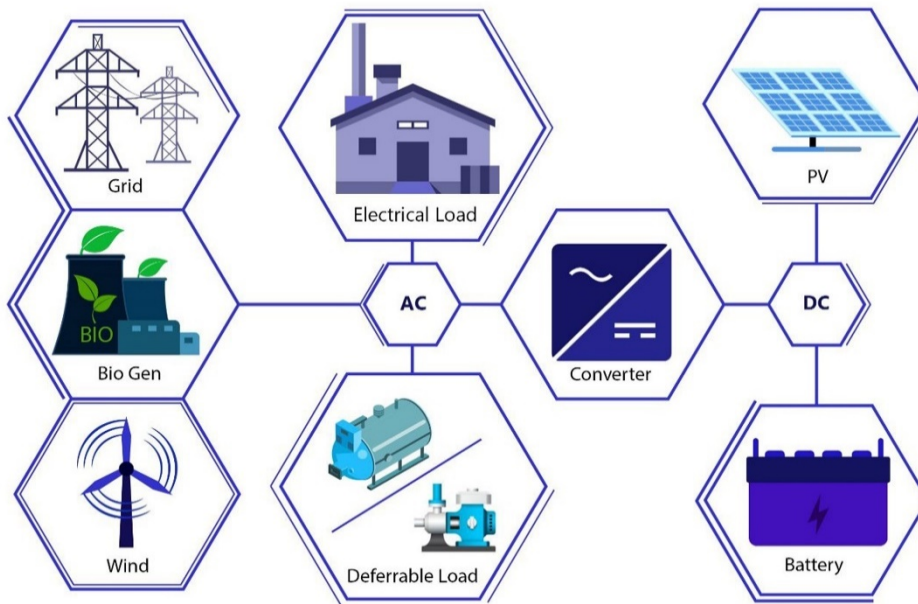


Figure 8. Schematic of the system which is going to supply energy demands of the factory

4.1. Photovoltaic panel

There is a limited space of 665 m² for installing the solar panels at the rooftop of the factor. Table 13 shows the characteristics and information of selected solar panels.

The solar panel data sheet also provides a chart that shows the warranted output during the operational years of the solar panel (Figure 9) [29].

Figure 9 indicates that installed solar panels will degrade 0.68 percent each year and will not have constant output during the lifetime of the project.

Table 13. Technical and economic information of selected photovoltaic panels

Name	Value	Unit	Ref.
Module type	TBM72-370M	-	[28]
Module dimension	1956 × 992 × 40	mm	
Maximum power (P _{max})	370	W	
Maximum voltage	39.59	V	
Maximum current	9.35	A	
Open-circuit voltage	48.04	V	
Short-circuit current	9.83	A	
Module efficiency	19.06	%	
Operating temp.	-40 ~ +85	°C	
Nominal module operating temperature	40.2 ± 2	°C	
Temp. coefficient of P _{max}	-0.39	-	
Capital and replacement cost per kW	1300	\$	[29]
O & M Cost	20	\$/yr	

4.2. Converter and electrical storage

In order to consume the DC output of solar panels and electrical storages (batteries) and store the AC output of biogas generator and wind turbines, the system uses converters to transform DC to AC, and vice versa. The output

of the converter also affects the output power of PVs as shown in Eq. 6 in Table 14 [24].

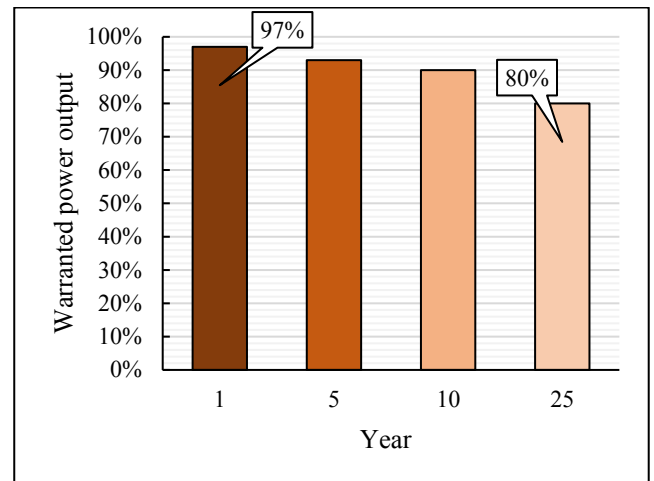


Figure 9. PV warranted output during 25 operational years [28]

Table 14. Converter output power equations

Equation	Eq. No.	Ref.
$P_{cnv.out} = \eta_{cnv} P_{PV}$	6	[24]

where η_{cnv} is equal to the efficiency of the converter and is assumed to be 90 %.

The optimization ability of HOMER pro software is used here and the values of 0, 50, 100, and 200 kW are chosen for converter to determine the best result for use in this project. Table 15 shows the summarized information of the converter.

Table 15. Summarized information of the installed converters

Component	Type	Simulation rates (kW)	Life time (yr)	Capital cost (\$)	Replacement cost (\$)	O & M (\$/yr)	Ref.
Converter	Generic	0, 50, 100, 200	15	600	600	10	[30]

Surrette 4 KS 25P flooded deep cycle battery is chosen in this study. Each of these batteries has a nominal capacity of 7.55 kWh and the corresponding values of 0, 20, and 50 are chosen for optimization. Data sheet of the selected batteries is shown in Table 16 [24].

Table 16. Technical data and information of Surrette 4 KS 25P battery

Name	Value	Unit	Ref.
Nominal voltage	4	V	[24]
Nominal capacity	1350	Ah	
Nominal capacity	7.55	kWh	
Life time	20	yr	[31]
Capital cost	1259	\$	
Replacement cost	1100	\$	
O & M cost	10	\$/yr	

shows the summarized technical and economic information of the selected wind turbines.

Table 17. Data sheet and economic information of wind turbines

Name	Value	Unit	Ref.
Rated power	10	kW	[11]
Life time	20	yr	
Capital cost	45000	\$	
Replacement cost	30000	\$	
O & M cost	500	\$/year	

Figure 10 shows the power curve of the chosen 10 kW wind turbine used in HOMER pro software for wind power simulations [32, 33].

4.4. Biogas generator

In order to use the potentials of biofuel resources, a biogas generator is used in the simulation. The capital cost for a biogas generator is 1500 \$/kW with the same value for its replacement, O & M cost of it is 60 \$/yr hour, and its life time is assumed to be 20,000 hours [29]. The main use of this biogas generator is for backup during the times that other

4.3. Wind turbine

Due to the average wind speed during past 22 years ranging between 5 and 8 m/s, generic wind turbines with the nominal capacity of 10 kW are used and the numbers of 0, 1, and 2 are chosen for optimizations in HOMER pro software. Table 17

renewable energies are not available to prevent the capacity shortages. Using a backup system will also reduce the use of

batteries, too. The values of 0, 10, 25, and 50 kW for biogas generator are used for optimization in HOMER pro software.

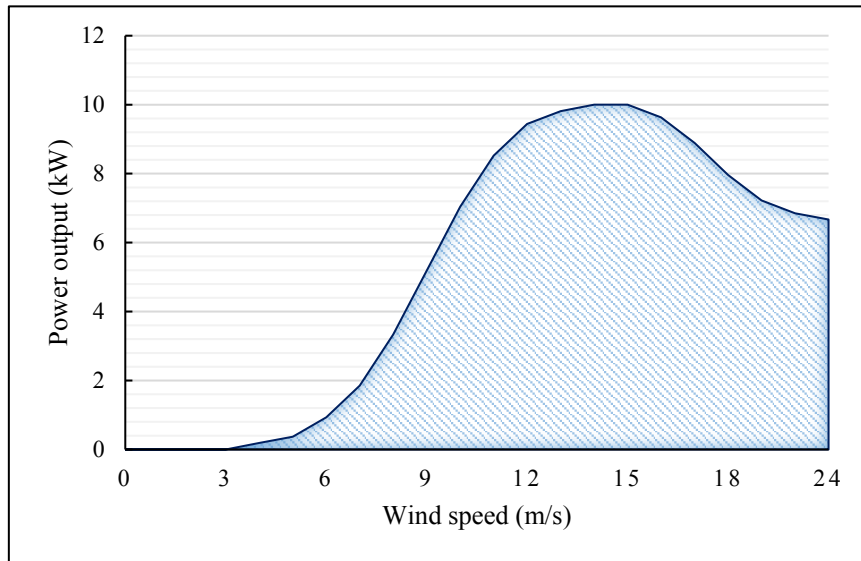


Figure 10. Power curve of generic 10 kW wind turbine [32]

5. PROJECT MANAGMENT

In this part, the paper will explain economics of the simulation and the effects of variable changes during the project life time.

5.1. Multi-year module

This module will help simulate the variable changes in the project during its life time and discuss its effects. Multi-year module is capable of simulating photovoltaic panel degradation and continuous changes in electrical loads (both primary and deferrable loads).

5.1.1. PV degradation

The photovoltaic panels will degrade 0.68 percent after each year and this will affect the investment of solar energy. In this case, the factory may need greater backup energy. To ensure that the simulation has enough insurance to be used in the real world, given that it is an industrial project and economic losses should be minimized, this degradation is considered in multi-year module of HOMER pro software.

5.1.2. Increase of electrical load

The increase in the electrical load of the factory is shown in the electrical consumption of the past three years in Table 3. This means that the project reaches the fifth year by the time, the electrical loads will be 1.5 times larger than their first value. By considering this increased amount of power consumption, the investors of hybrid renewable energies can make sure that their factories will no longer have the problem of future capacity shortages.

5.2. Economics and sensitivity module

The life time of this industrial project is assumed to be 25 years. At the time of writing this paper, the nominal discount rate is 18 % and the inflation rate is 15 % [24]. However, it is possible that these values of discount rate and inflation rate change during the project life time [34]. In this case, the sensitivity module of HOMER pro software is employed to analyze the future possibilities and plan for them. The average 5 % of changes for each of these economic parameters is assumed [35]. Table 18 shows the summarized information of the assumptions of project management part in the simulations.

Table 18. Assumptions of the project management part in the simulations

Name	Project life time (year)	Nominal discount rate (%)	Expected inflation rate (%)	PV degradation (%/yr)	Increase of loads until year 5 (%/yr)
Value	25	13, 18, 23	10, 15, 20	0.68	10

6. RESULTS AND DISCUSSION

Summarized results of both off-grid and on-grid scenarios are shown in Table 19.

6.1. Grid-connected system

The advantage of using grid-connected systems is that there is a possibility to sell the surplus energy to the grid at non-peak hours and at times when the factory is not operational and yet, the components and the system are producing electricity using

renewable energy resources. Selling the surplus green energy will provide both economic and environmental profits.

Among the optimal on-grid systems that are shown in Table 19, the application of photovoltaic panels without the use of wind turbines and biogas generator in Scenario 1 has the lowest NPC, COE, and initial capital cost and can be chosen as the most economic system. In order to show the costs of the system in Scenario 1 in detail, a chart is established and shown Figure 11.

Operation of the solar panels is important, especially due to the changes that are programmed in the multi-year module. Figure 12 shows the PV output during a day in its initial state

in the 1st year and Table 20 compares this initial state with 5th, 10th, and 25th years of the project.

Table 19. Best results of off-grid and on-grid scenarios (present inflation and discount rates)

Scenario		Components					Grid		Costs		
		PV (kW)	Wind turbine (Qty.)	Bio Gen. (kW)	Battery (Qty.)	Converter (kW)	Purchased (kWh)	Sold (kWh)	NPC (\$)	COE (\$)	Initial capital (\$)
On-grid	1	100	-	-	20	50	31,693	63,489	200,415	0.070	195,180
	2	100	-	10	20	50	31,693	63,493	207,729	0.072	210,180
	3	100	1	-	50	50	26,995	72,154	231,476	0.076	240,780
Off-grid	1	100	2	25	50	50	-	-	597,970	0.35	360,450
	2	100	-	25	50	50	-	-	651,058	0.38	270,450
	3	100	2	50	-	50	-	-	9.25 M	5.42	335,000

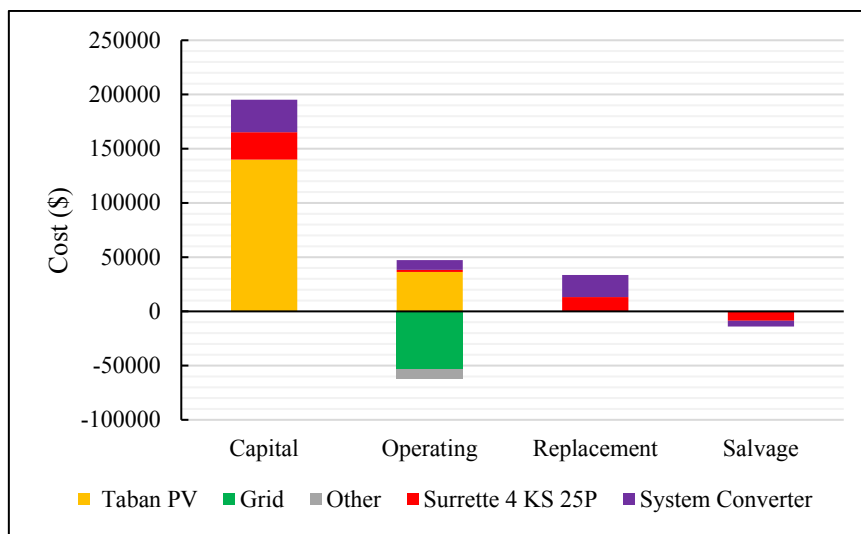


Figure 11. Cost summary of the optimum on-grid system (PV/battery/grid)

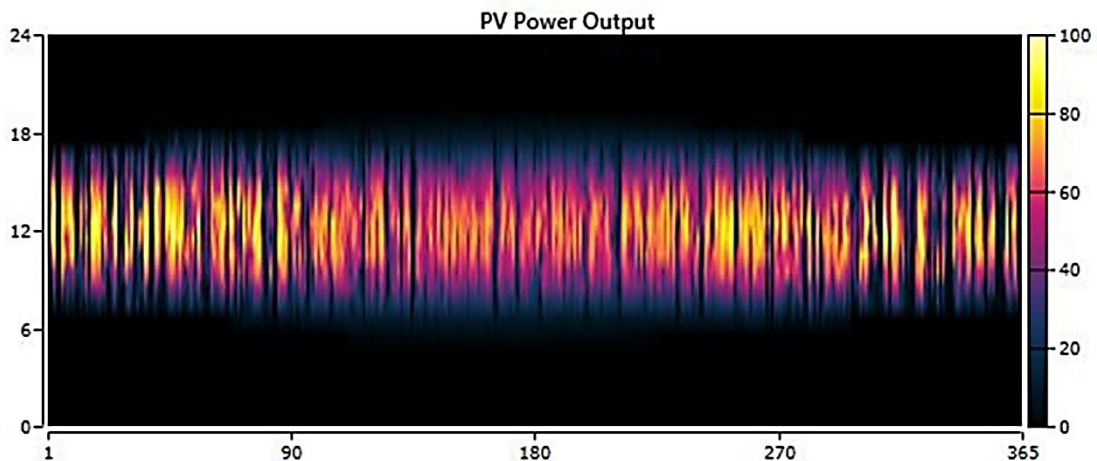


Figure 12. PV power output in its initial state in year 1

Table 20. Compression between the states of PVs during the project life time

Year	Maximum output (kW)	PV penetration (%)	Levelized cost (\$/kWh)	Total production (kWh/yr)
1	98.2	250	0.061	158,254
5	95.6	162	0.063	153,994
10	92.4	157	0.065	148,829
25	83.4	142	0.072	134,350

According to Table 20, PV penetration experienced a significant reduction after 5 years and reached the amount of 162 % from its initial value (250 %) due to increase in primary and deferrable loads of the factory. However, even after this time, degradation of PV panels during the project life time has a considerable effect on its penetration and electricity production. The total reduction in the production of PVs is near 24,000 kWh/yr. The amount power that the factory consumes from grid during the day when the factory is operational is also affected by PV degradation, as shown in Figure 13.

Figure 13 shows the effects of PV degradation on grid status and explains how it influences needed power and the way that the system works. Comparison of the 1st year and last year of the project indicates that the amount of excess energy that can be sold to the grid is reduced at the 25th year and also, greater energy is purchased from the grid during the final hours of the day.

The optimal system can be different for each economic condition and the sensitivity analysis has the ability to indicate each one clearly. Figure 14 shows the optimal system type for each economic condition and the effect of both inflation and discount rates on the operating hybrid renewable energy system type.

On-grid results shown in Table 19 are at the center of Figure 14; however, higher discount rate (more than 20 %) and lower inflation rate (lower than 13 %) will prompt the system to use biogas generators instead of using PVs. Reduction of discount rate will also make the system use PVs and biogas energy together. There is also a small chance that the system uses biogas generator, PV, and wind turbine together if the inflation rate reaches the value of 20 % while the discount rate is 13 %. Fluctuations of inflation and discount rates also affect the NPC of the project and these effects are shown in a surface plot in Figure 15.

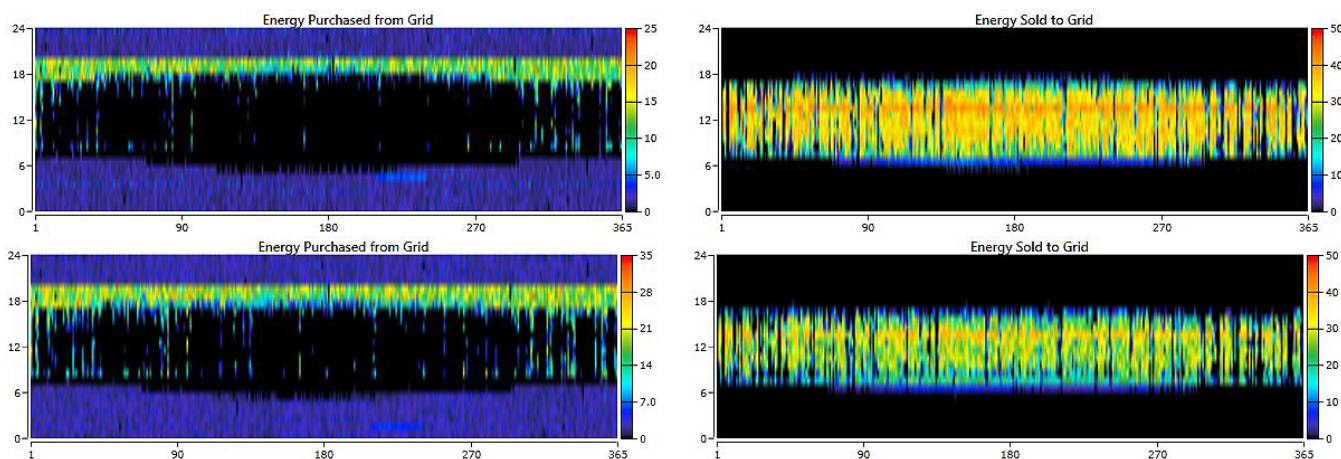


Figure 13. Grid status during the project life time (up: 1st year, down: 25th year)

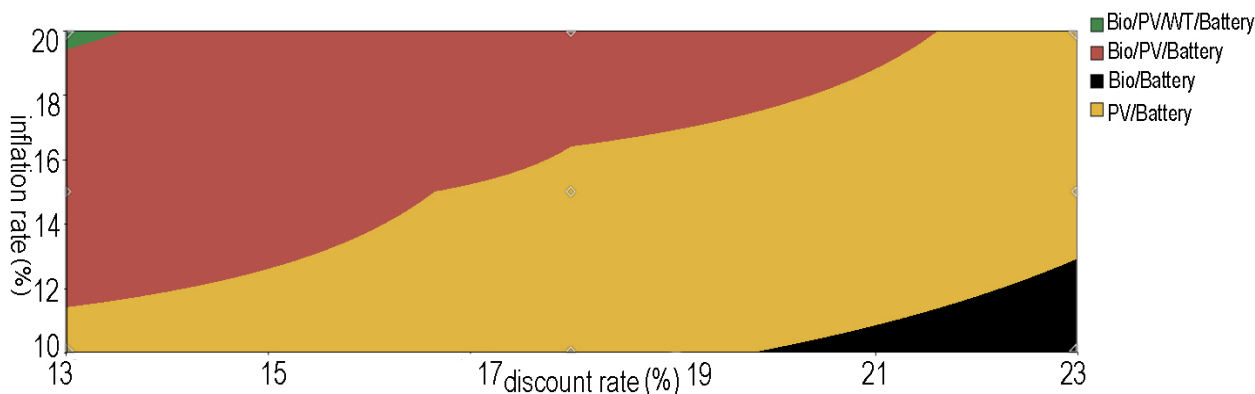


Figure 14. Optimal system type for each economic condition (on-grid system)

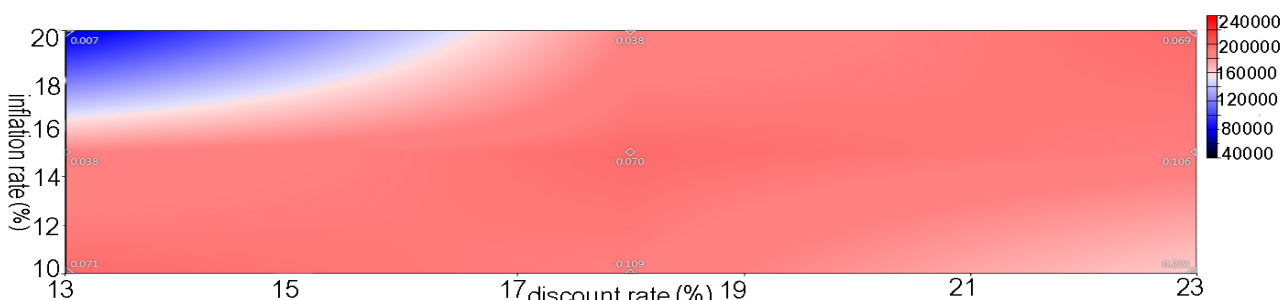


Figure 15. Surface plot of Net Present Cost in the grid-connected scenario

The surface plot of NPC indicates that lower discount and higher inflation will lead to reduced NPC and COE and the inflation rate of 20 % and discount rate of 13 % have the lowest NPC and COE, which belong to the PV/bio/WT/battery system. The inflation rate of 10 % and the discount rate of 23 % also reduce the NPC while creating the highest COE.

In addition to optimum system type, NPC, and COE, economic fluctuations can also affect the emissions. Figure 16

shows the effects of inflation rate and discount rate on CO₂ emissions and the environmental effects of this project.

Figure 16 indicates that when the inflation rate increases and discount rate decreases, the bio/battery system will produce carbon emissions while other optimum systems of the factory are all negative-carbon producers. CO₂ emissions of the on-grid system vary between -60,000 kg/yr and 90,000 kg/yr.

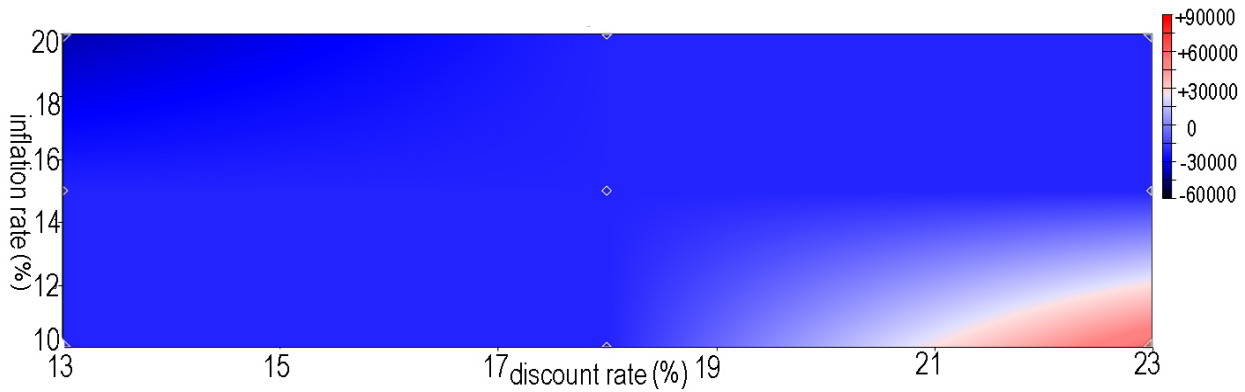


Figure 16. Surface plot of average CO₂ emissions per year in the grid-connected scenario

6.2. Stand-alone system

In this part, this paper attempts to analyze the stand-alone system to determine what it will take to make an industrial factory off-grid and use total renewable energies to make it become a green factory. Cost summary for the optimum off-grid scenario involving the present inflation rate and discount rate is shown in Figure 17.

As is given in Figure 17, the largest capital cost in this scenario belongs to PVs followed by wind turbines, given that the lifetime of the project is 25 years.

In this scenario, wind turbines and biogas generator should be analyzed as new components of the system in the off-grid mode. Figure 18 shows the status and production of wind turbines in the off-grid system.

Degradation of PV panels (24,000 kWh drop in total production) and increase of electrical loads have greater effects on this scenario as the factory does not have the support of the grid power. In this case, wind turbines and biogas generator should produce enough electricity to keep the factory operational. Table 21 shows the status of biogas generator and biofuel consumption during the project lifetime.

According to Table 21, the operational hours of biogas generator and its production increase after 5 years due to a 10 % increase in electrical loads of the factory. Comparison of the scenarios indicates that the degradation of the PVs leads the system to use more biogas after each year in the off-grid scenario. PV degradation itself leads the system to increase the use of biogas generator. The amount of biogas consumption reaches 9330 kg/yr in the 25th year from 7260 kg/yr in the 5th year of the project.

Lack of grid power forces the system to use more batteries, and 30 batteries are added to the stand-alone system to make sure that it is going to meet capacity shortages. Figure 19 shows the status of batteries in the stand-alone system in the 1st, 10th, and 25th years from top to down, respectively.

Figure 19 indicates that effects of the continuous changes that are simulated in the multi-year module on the storage system. As the project progresses, the system uses more stored energy to supply the factory.

Figure 20 shows the results of sensitivity analysis in off-grid system types, and Figure 21 shows the effects of inflation rate and discount rate on the economic parameters of the project.

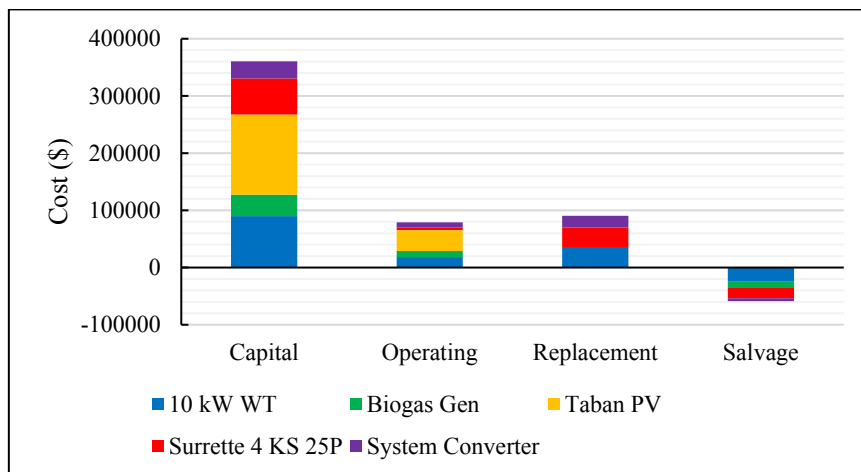


Figure 17. Cost summary for the optimum off-grid system (PV/WT/bio/battery)

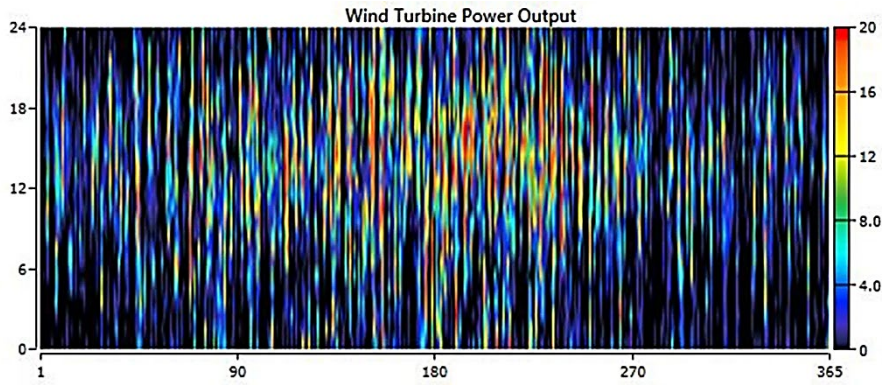


Figure 18. Wind turbine output during one year (off-grid scenario)

Table 21. Status of biogas generator during the project lifetime (off-grid scenario)

Year	Hours of operation (hrs/yr)	Number of starts (Qnt/yr)	Electrical production (kWh/yr)	Biogas consumption (kg/yr)
1	27	17	338	742
5	248	127	3320	7260
10	267	130	3561	7789
25	315	154	4271	9330

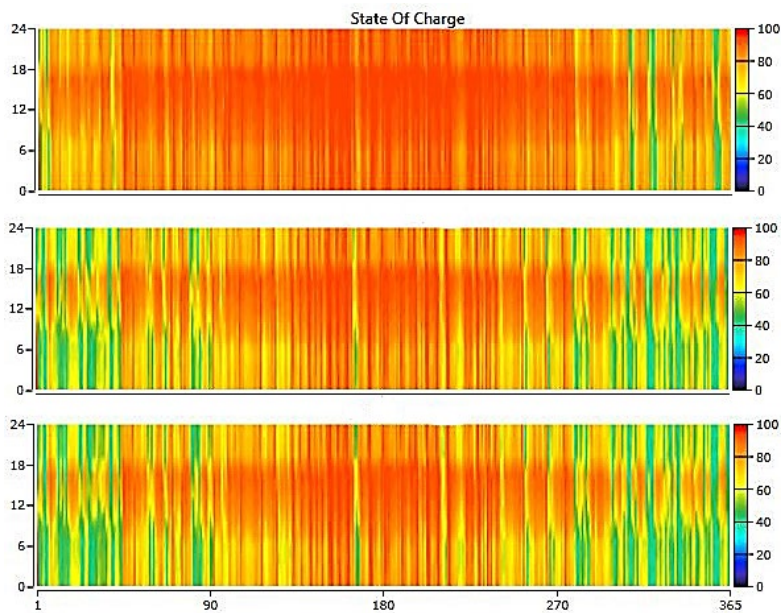


Figure 19. Status of batteries during 1st, 10th, and last years (from top to down, respectively)



Figure 20. Surface plot of optimal system type in the off-grid scenario

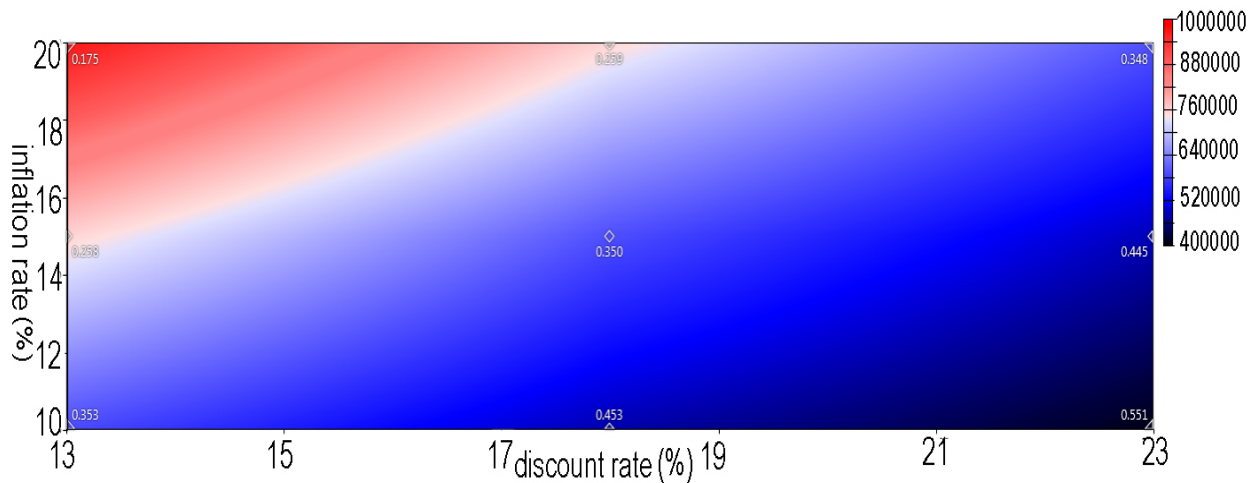


Figure 21. Surface plot of NPC in the off-grid scenario

The center of Figure 20 shows the current status of the stand-alone system; however, when the discount rate increases and the inflation rate decreases, the system will delete wind turbines and avoid using them. The center of the NPC surface plot (Figure 21) also shows the status of the present investment and changes in NPC and COE are predicted to help the factory to decide whether this is affordable to use this project or not. Comparison of the scenarios explains that inflation rate and discount rate fluctuations have significant effects on the stand-alone scenario, compared to the grid-

connected scenario. Environmental effects of economic fluctuations are also shown in a surface plot in Figure 22.

Unlike the on-grid scenario, the off-grid system cannot become a negative-carbon producer as it is not connected to the grid and cannot sell the surplus green energy. Carbon emission of the stand-alone system only varies between 500 kg/yr and 1100 kg/yr. However, the amount of carbon emissions produced by the on-grid system will significantly change and increase when inflation rate decreases and discount rate decreases.

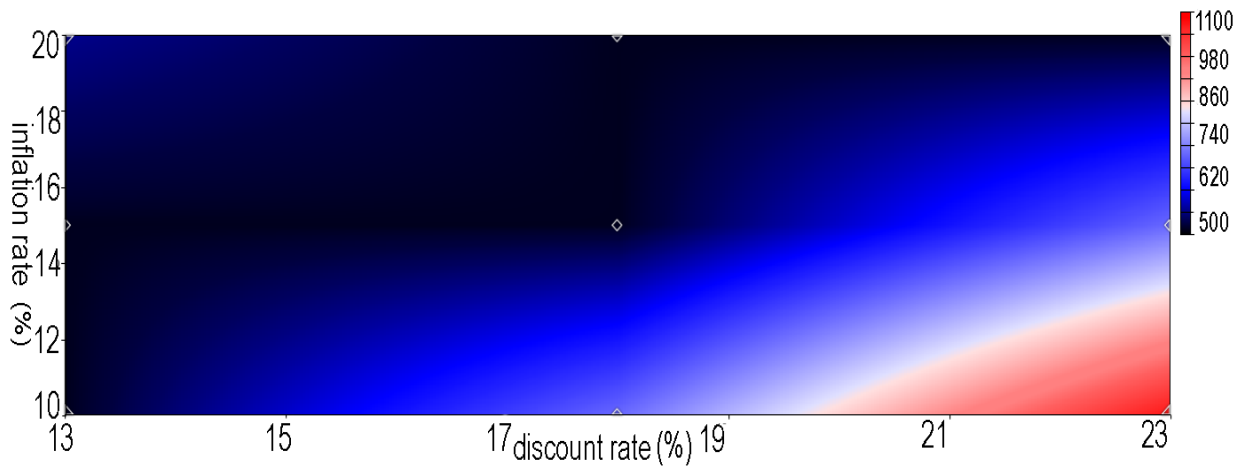


Figure 22. Surface plot of average CO₂ emissions per year in the stand-alone scenario

6.3. Multi-year/single-year compression

The results and effects of using the multi-year module on the whole project consisting of the changes of the optimum system type, NPC, COE, and carbon emissions are analyzed and reported in this part. Effect of economic fluctuations without enabling multi-year module in the simulations on the optimum system type of the grid-connected system is shown in a surface plot in Figure 23.

According to Figure 23, effects of fluctuations of inflation and discount rates while multi-year module is disabled creates four different optimum systems. The optimum systems shown in Figure 23 totally differ from those that are obtained in Figure 14. Although the present system at the center of Figure 23 is the same as the one in Figure 14 (PV/battery), using multi-year module of HOMER pro software significantly affects the installed systems in other economic conditions.

Increasing the inflation rate deletes the battery component in the single-year model and adds the biogas generator. If the inflation rate reaches 16 % and discount rate decrease to 15 %, batteries will be added to the PV/bio system again. Stand-alone system is no exception and disabling the multi-year module will affect the optimum system type of it, too. Effect of economic fluctuations while the multi-year module is not enabled on the off-grid system is shown in Figure 24.

Figure 24 indicates that disabling the multi-year module will delete the wind turbine component in the present condition. The wind turbine can only be added to the bio/PV/battery system if the inflation rate reaches 19 % and discount rate goes under 14 %. Table 22 compares the amount of NPC and COE of the multi-year mode with those in the single-year mode. Note that this compression belongs to the present inflation rate and discount rate.

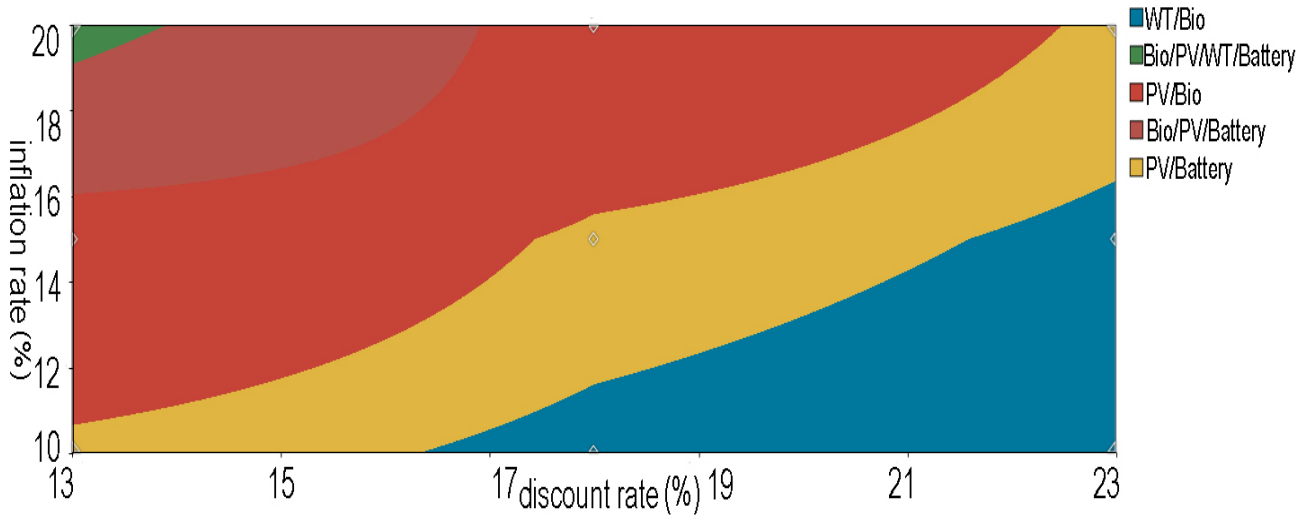


Figure 23. Surface plot of the optimum system type while the multi-year module is disabled (on-grid mode)

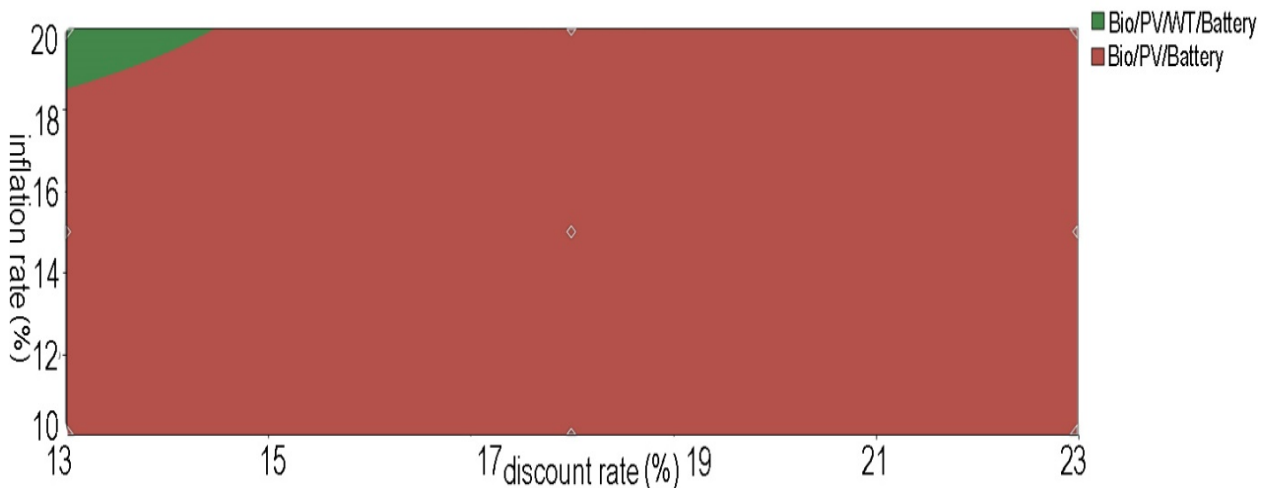


Figure 24. Surface plot of the optimum system type while the multi-year module is disabled (off-grid mode)

Table 22. Multi-year module effects on NPC and COE

Parameter	Multi-year	Grid-connected	Stand-alone	Unit
NPC	■	200,415	597,970	\$
NPC	□	144,620	371,074	\$
COE	■	0.07	0.35	\$/kWh
COE	□	0.0528	0.314	\$/kWh

The difference between the NPCs of the grid-connected system between the multi-year mode and the single-year mode, which is shown in Table 22, is 55,795 \$. For the stand-alone system, the amount of difference is equal to 226,896 \$. From this difference between the NPC values, it can be obtained that using the multi-year module of the HOMER pro software improved the simulations by adding greater accuracy to them. In addition to economic parameters, emissions can also be analyzed more accurately. Carbon emission trend of designed energy hubs for both single-year and multi-year modes is shown in Figure 25 (Present inflation rate and discount rate).

Changing the CO₂ emission during the project life time due to PV degradation and changes of electrical loads is clear in Figure 25. Further, by disabling the multi-year module, CO₂ emission of both on-grid and off-grid systems remains a constant value. The grid-connected system saves 43,819 kg of CO₂ per year. By enabling the multi-year module, this value will change as the project progresses and will reach 14,673 kg/yr in the last year. The stand-alone system only emits 149 kg/yr in the single-year mode. However, by employing the multi-year module of HOMER pro software, the amount of emitted CO₂ in the off-grid system will increase and reach 655 kg/yr in the 25th year of the project.

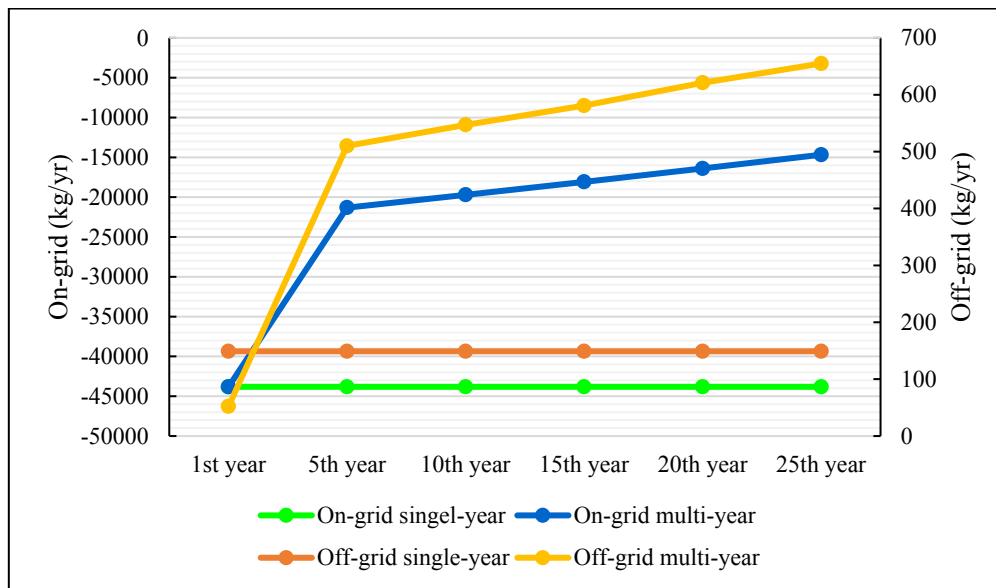


Figure 25. Effects of the multi-year module on the carbon emission trend of the system

7. CONCLUSIONS

This paper, for the first time, aimed to investigate the use of green energies in factories and industrial projects by considering the industrial deferrable load, changes in electrical load, degradation of components, and economic fluctuations. Most factories use air compressors and pumps in their production lines. The most important results of this research are given as follows:

- Increasing the electrical consumption of the factory and degradation of PVs together reduces the solar energy penetration from 250 % in the 1st year to 142 % in the last year and also, increases the levelized cost of solar energy from 0.061 \$/kWh in the beginning of the project to 0.072 \$/kWh in the 25th year (optimum grid-connected scenario).
- Increasing the electrical loads of the factory and reducing solar panels production can increase the use of biogas from 742 kg/yr at the beginning of the project to 9330 kg/yr at the end of the project. The electrical production of the biogas generator also reaches 4271 kWh/yr in the 25th year from 338 kWh/yr in the 1st year.
- Economic fluctuations lead the simulation to choose two off-grid systems: PV/bio/WT/battery and PV/bio/battery.
- Fluctuations of economics do not have considerable effects on carbon emissions of stand-alone systems, but may significantly increase the carbon emissions of on-grid systems.
- Comparison of the single-year mode and multi-year mode indicates that disabling the multi-year module will totally change optimum system types of both on-grid and off-grid systems. However, the present grid-connected system will remain a PV/battery system, while the optimum stand-alone system will be changed into PV/bio/battery.

8. ACKNOWLEDGEMENT

The authors like to thank the managers of the KSJ factory for their cooperation and providing data for the research.

This research did not receive any specific grant from funding agencies in the public, commercial, or not-for-profit sectors.

NOMENCLATURE

Bat	Battery
BG	Biogas generator
COE	Cost of Energy (\$/kWh)
DG	Diesel generator
eLAN	Energy local area network
FC	Fuel cell
HE	Hydro Electric
HSPSI	Pumped Storage
KSJ	Name of the Case Study Factory
NOCT	Nominal Operating Cell Temperature (°C)
NPC	Net Present Cost (\$)
O & M	Operating and Maintenance
OC	Operating Cost (\$)
PV	Photovoltaic
STC	Standard Test Condition
WT	Wind Turbine

Greek letters

τ	Solar transmittance of the cover over PV array (%)
μ	temperature coefficient (-)

REFERENCES

1. Bukar, A.L. and Tan, C.W., "A review on stand-alone photovoltaic-wind energy system with fuel cell: System optimization and energy management strategy", *Journal of Cleaner Production*, Vol. 221, (2019), 73-88. (<https://doi.org/10.1016/j.jclepro.2019.02.228>).
2. Akikur, R.K., Saidur, R., Ping, H.W. and Ullah, K.R., "Comparative study of stand-alone and hybrid solar energy systems suitable for off-grid rural electrification: A review", *Renewable and Sustainable Energy Reviews*, Vol. 27, (2013), 738-752. (<https://doi.org/10.1016/j.rser.2013.06.043>).
3. Haddad, A., Ramadan, M., Khaled, M., Ramadan, H. and Becherif, M., "Study of hybrid energy system coupling fuel cell, solar thermal system and photovoltaic cell", *International Journal of Hydrogen*, Vol. 45, No. 25, (2020), 13564-13574. (<https://doi.org/10.1016/j.ijhydene.2018.06.019>).
4. Xu, X., Hu, W., Cao, D., Huang, Q., Chen, C. and Chen, Z., "Optimized sizing of a standalone PV-wind-hydropower station with pumped-storage installation hybrid energy system", *Renewable Energy*, Vol. 147, Part 1, (2020), 1418-1431. (<https://doi.org/10.1016/j.renene.2019.09.099>).
5. Ribó-Pérez, D., Herraiz-Cañete, Á., Alfonso-Solar, D., Vargas-Salgado, C. and Gómez-Navarro, T., "Modelling biomass gasifiers in hybrid

- renewable energy microgrids: A complete procedure for enabling gasifiers simulation in HOMER", *Renewable Energy*, Vol. 174, (2021), 501-512. (<https://doi.org/10.1016/j.renene.2021.04.083>).
6. Purlu, M., Beyarslan, S. and Turkay, B.E., "Optimal design of hybrid grid-connected microgrid with renewable energy and storage in a rural area in Turkey by using HOMER", *Proceedings of 13th International Conference on Electrical and Electronics Engineering (ELECO)*, IEEE, (2021), 263-267. (<https://doi.org/10.23919/ELECO54474.2021.9677788>).
 7. De la Cruz-Soto, J., Azkona-Bedia, I., Velazquez-Limon, N. and Romero-Castanon, T., "A techno-economic study for a hydrogen storage system in a microgrid located in baja California, Mexico. Levelized cost of energy for power to gas to power scenarios", *International Journal of Hydrogen Energy*, Vol. 47, No. 20, (2022), 30050-30061. (<https://doi.org/10.1016/j.ijhydene.2022.03.026>).
 8. Jahangir, M.H., Montazeri, M., Mousavi, S.A. and Kargarzadeh, A., "Reducing carbon emissions of industrial large livestock farms using hybrid renewable energy systems", *Renewable Energy*, Vol. 189, (2022), 52-65. (<https://doi.org/10.1016/j.renene.2022.02.022>).
 9. Shakya, S.R., Bajracharya, I., Vaidya, R.A., Bhave, P., Sharma, A., Rupakheti, M. and Bajracharya, T.R., "Estimation of air pollutant emissions from captive diesel generators and its mitigation potential through microgrid and solar energy", *Energy reports*, Vol. 8, (2022), 3251-3262. (<https://doi.org/10.1016/j.egyr.2022.02.084>).
 10. Roth, A., Boix, M., Gerbaud, V., Montastruc, L. and Etur, P., "A flexible metamodel architecture for optimal design of Hybrid Renewable Energy Systems (HRES)–Case study of a stand-alone HRES for a factory in Tropical Island", *Journal of Cleaner Production*, Vol. 223, (2019), 214-225. (<https://doi.org/10.1016/j.jclepro.2019.03.095>).
 11. Ogunjuyigbe, A. and Ayodele, T., "Techno-economic analysis of stand-alone hybrid energy system for Nigerian telecom industry", *International Journal of Renewable Energy Technology*, Vol. 7, No. 2, (2016), 148-162. (<https://www.inderscienceonline.com/doi/abs/10.1504/IJRET.2016.076089>).
 12. Diab, F., Lan, H., Zhang, L. and Ali, S., "An environmentally friendly factory in Egypt based on hybrid photovoltaic/wind/diesel/battery system", *Journal of Cleaner Production*, Vol. 112, Part 5, 3884-3894. (<https://doi.org/10.1016/j.jclepro.2015.07.008>).
 13. Al-Ghussain, L., Ahmed, H. and Haneef, F., "Optimization of hybrid PV-wind system: Case study Al-Tafilah cement factory, Jordan", *Sustainable Energy Technologies and Assessments*, Vol. 30, (2018), 24-36. (<https://doi.org/10.1016/j.seta.2018.08.008>).
 14. Makhija, S.P. and Dubey, S., "Feasibility analysis of biomass-based grid-integrated and stand-alone hybrid energy systems for a cement plant in India", *Environment, Development and Sustainability*, Vol. 21, No. 2, (2019), 861-878. (<https://doi.org/10.1007/s10668-017-0064-0>).
 15. Mirzaei, M. and Vahidi, B., "Feasibility analysis and optimal planning of renewable energy systems for industrial loads of a dairy factory in Tehran, Iran", *Journal of Renewable and Sustainable Energy*, Vol. 7, No. 6, (2015), 063114. (<https://doi.org/10.1063/1.4936591>).
 16. Shezan, S.A., Julai, S., Kibria, M., Ullah, K., Saidur, R., Chong, W. and Akikur, R., "Performance analysis of an off-grid wind-PV (photovoltaic)-diesel-battery hybrid energy system feasible for remote areas", *Journal of Cleaner Production*, Vol. 125, 121-132. (<https://doi.org/10.1016/j.jclepro.2016.03.014>).
 17. HOMER, Designing of the deferrable load, (2020). (https://www.homerenergy.com/products/pro/docs/latest/deferrable_load.html), (Accessed 29 March 2020).
 18. Izadyar, N., Ong, H.C., Chong, W.T., Mojumder, J.C. and Leong, K., "Investigation of potential hybrid renewable energy at various rural areas in Malaysia", *Journal of Cleaner Production*, Vol. 139, (2016), 61-73. (<https://doi.org/10.1016/j.jclepro.2016.07.167>).
 19. Singh, A., Baredar, P. and Gupta, B., "Techno-economic feasibility analysis of hydrogen fuel cell and solar photovoltaic hybrid renewable energy system for academic research building", *Energy Conversion and Management*, Vol. 145, (2017), 398-414. (<https://doi.org/10.1016/j.enconman.2017.05.014>).
 20. Mandal, S., Das, B.K. and Hoque, N., "Optimum sizing of a stand-alone hybrid energy system for rural electrification in Bangladesh", *Journal of Cleaner Production*, Vol. 200, (2018), 12-27. (<https://doi.org/10.1016/j.jclepro.2018.07.257>).
 21. Zahboune, H., Zouggar, S., Krajačić, G., Varbanov, P.S., Elhafyani, M. and Ziari, E., "Optimal hybrid renewable energy design in autonomous system using Modified Electric System Cascade Analysis and Homer software", *Energy Conversion and Management*, Vol. 126, 909-922. (<https://doi.org/10.1016/j.enconman.2016.08.061>).
 22. Sarkar, T., Bhattacharjee, A., Samanta, H., Bhattacharya, K. and Saha, H., "Optimal design and implementation of solar PV-wind-biogas-VRFB storage integrated smart hybrid microgrid for ensuring zero loss of power supply probability", *Energy Conversion and Management*, Vol. 191, (2019), 102-118. (<https://doi.org/10.1016/j.enconman.2019.04.025>).
 23. Belfkira, R., Zhang, L. and Barakat, G., "Optimal sizing study of hybrid wind/PV/diesel power generation unit", *Solar Energy*, Vol. 85, No. 1, (2011), 100-110. (<https://doi.org/10.1016/j.solener.2010.10.018>).
 24. Hanafizadeh, P., Eshraghi, J., Ahmadi, P. and Sattari, A., "Evaluation and sizing of a CCHP system for a commercial and office buildings", *Journal of Building Engineering*, Vol. 5, (2016), 67-78. (<https://doi.org/10.1016/j.jobbe.2015.11.003>).
 25. Jahangir, M.H., Javanshir, F. and Kargarzadeh, A., "Economic analysis and optimal design of hydrogen/diesel backup system to improve energy hubs providing the demands of sport complexes", *International Journal of Hydrogen Energy*, Vol. 46, No. 27, (2021), 14109-14129. (<https://doi.org/10.1016/j.ijhydene.2021.01.187>).
 26. Halabi, L.M., Mekhilef, S., Olatomiwa, L. and Hazelton, J., "Performance analysis of hybrid PV/diesel/battery system using HOMER: A case study Sabah, Malaysia", *Energy Conversion and Management*, Vol. 144, (2017), 322-339. (<https://doi.org/10.1016/j.enconman.2017.04.070>).
 27. Poeschl, M., Ward, S. and Owende, P., "Prospects for expanded utilization of biogas in Germany", *Renewable and Sustainable Energy Reviews*, Vol. 14, No. 7, (2010), 1782-1797. (<https://doi.org/10.1016/j.rser.2010.04.010>).
 28. IRENA, Biogas Cost Reductions to Boost Sustainable Transport, (2017). (<https://www.irena.org/newsroom/articles/2017/Mar/Biogas-Cost-Reductions-to-Boost-Sustainable-Transport>), (Accessed 7 April 2020).
 29. Taban, e.d.c., PERC Mono Crystalline 72 Cell Module, (2019). (<https://tabanenergy.ir/wp-content/pdf/catalogue5BB-Mono-Feb2019.pdf>), (Accessed 16 April 2020).
 30. Mohammadi, M., Ghasempour, R., Astaraei, F.R., Ahmadi, E., Aligholian, A. and Toopshekan, A., "Optimal planning of renewable energy resource for a residential house considering economic and reliability criteria", *International Journal of Electrical Power & Energy Systems*, Vol. 96, 261-273. (<https://doi.org/10.1016/j.ijepes.2017.10.017>).
 31. Rad, M.A.V., Ghasempour, R., Rahdan, P., Mousavi, S. and Arastounia, M., "Techno-economic analysis of a hybrid power system based on the cost-effective hydrogen production method for rural electrification, a case study in Iran", *Energy*, Vol. 190, (2020), 116421. (<https://doi.org/10.1016/j.energy.2019.116421>).
 32. Li, C., Zhou, D. and Zheng, Y., "Techno-economic comparative study of grid-connected PV power systems in five climate zones, China", *Energy*, Vol. 165, Part B, (2018), 1352-1369. (<https://doi.org/10.1016/j.energy.2018.10.062>).
 33. Gökçek, M., "Integration of hybrid power (wind-photovoltaic-diesel-battery) and seawater reverse osmosis systems for small-scale desalination applications", *Desalination*, Vol. 435, (2018), 210-220. (<https://doi.org/10.1016/j.desal.2017.07.006>).
 34. Aziz, A.S., Tajuddin, M.F.N., Adzman, M.R., Azmi, A. and Ramli, M.A., "Optimization and sensitivity analysis of standalone hybrid renewable energy systems for rural electrification: A case study of Iraq", *Renewable Energy*, Vol. 138, 775-792. (<https://doi.org/10.1016/j.renene.2019.02.004>).
 35. Shahzad, M.K., Zahid, A., ur Rashid, T., Rehan, M.A., Ali, M. and Ahmad, M., "Techno-economic feasibility analysis of a solar-biomass off grid system for the electrification of remote rural areas in Pakistan using HOMER software", *Renewable Energy*, Vol. 106, 264-273. (<https://doi.org/10.1016/j.renene.2017.01.033>).